Thin Solid Films 612 (2016) 96–100

Contents lists available at ScienceDirect

Thin Solid Films

journal homepage: www.elsevier.com/locate/tsf

Mechanism and model of atomic hydrogen cleaning for different types of carbon contamination on extreme ultraviolet multilayers

Yuan Song [a,b], Qipeng Lu [a,*], Xuepeng Gong [a]

[a] State Key Laboratory of Applied Optics, Changchun Institute of Optics, Fine Mechanics and Physics, Chinese Academy of Sciences, Changchun, Jilin 130033, China
[b] University of Chinese Academy of Sciences, Beijing 100049, China

ARTICLE INFO

Article history:
Received 11 November 2015
Received in revised form 13 May 2016
Accepted 2 June 2016
Available online 3 June 2016

Keywords:
Atomic hydrogen cleaning
Different types of carbon contamination
Extreme ultraviolet lithography
Cleaning mechanism

ABSTRACT

The use of atomic hydrogen to clean carbon contaminants on multilayers in extreme ultraviolet lithography systems has been extensively investigated. Additional knowledge of the cleaning rate would not only provide a better understanding of the reaction mechanism but would also inform the industry's cleaning process. In this paper, which focuses on the atomic-hydrogen-based carbon contamination cleaning process, a possible mechanism for the associated reactions is studied and a cleaning model is established. The calculated results are in good agreement with the existing experimental data in the literature. The influences of the main factors – such as activation energy and types of contamination – on the cleaning rate are addressed by the model. The model shows that the cleaning rate depends on the type of carbon contamination. The rate for a polymer-like carbon layer is higher than the rate for graphitic and diamond-like carbon layers. At 340 K, the rate for a polymer-like carbon layer is 10 times higher than for graphitic carbon layers. This model could be used effectively to predict and evaluate the cleaning rates for various carbon contamination types.

1. Introduction

Extreme ultraviolet lithography (EUVL) is a developing lithography technology at the 11–22-nm node and its use is likely to increase in the future [1,2]. The prototype produced by ASML, EUVL NEX: 3300B, can produce 600 wafers per day as of 2015. The commercial model EUVL NEX: 3305B, which is expected to be available in 2016, will produce 1500 wafers per day. During EUV exposure, the remaining hydrocarbons in the surroundings deposit on the surface of optical elements and inevitably generate carbon contamination under EUV source illumination. These contaminants absorb EUV light, which leads to the loss of reflectance. For a commercial EUVL, the loss in reflectance should be less than 1.6% during the lifetime of the optical system, which is usually more than 30,000 h. This requirement means that the thickness of the carbon contaminant layer must remain less than 2 nm [3,4]. Therefore, removing carbon contaminants can prolong the service life of EUVL systems.

There are several ways to clean the carbon contamination, such as Radio Frequency (RF)–O_2/H_2, UV/O_2, EUV/O_2 and atomic hydrogen [5–8]. Atomic hydrogen is considered to have the most potential for removing carbon contaminants on EUV multilayers because it causes little oxidation or other damage to the surface of the multilayer. The cleaning rate is an important technical index for evaluating cleaning methods. Due to the effects of EUV irradiation flux, surrounding conditions, and other factors, the types of carbon contamination generated on the EUV optical elements vary, as do their cleaning rates. Graham and his colleague have obtained a 0.1 nm/min cleaning rate for sputtering deposition induced carbon and a 0.2 nm/min rate for EUV-induced carbon in their experiments [5].

To elucidate the cleaning process for different types of contamination and predict their associated cleaning rates, it is necessary to develop an accurate model. At present, there is no clear model based on chemical kinetics to explain the cleaning process. In this paper, a possible mechanism for the reactions is studied and a cleaning model is established. The influences of the main factors – such as activation energy and types of contamination – on the cleaning process and the cleaning rate are discussed. The calculated results are in good agreement with the existing experimental data in the literature. This model could be used effectively to predict and evaluate the cleaning rates for different carbon contamination types and inform the industry cleaning process.

2. Types of carbon contaminants on EUV multilayers

The types of carbon contaminants on EUV multilayers vary with changes in surface exposure intensity, temperature, background gases, exposure time and so on [9]. Main types of carbon contaminants are polymer-like, diamond-like and graphite-like. The types are usually determined by XPS [10], but this method is inconvenient. This paper

* Corresponding author.
E-mail address: Luqipeng51@126.com (Q. Lu).

http://dx.doi.org/10.1016/j.tsf.2016.06.002
0040-6090/

studies the relationship between the types and the reflectivity losses for use as a method to determine contaminant type. We assumed that the sample is a standard EUV multilayer mirror consisting of 50 thin bilayers of Mo and Si deposited on a Si (100) wafer with a 2-nm-thick cap layer of Ru subsequently deposited on top. We calculated the reflectivity of multilayers for different types of carbon contamination; as shown in Fig. 1, the reflectivity of the multilayers depends on the contaminant type.

The reflectivity of a standard Mo/Si multilayer is 75.53% at a wavelength of 13.5 nm and decreases with the deposition of different types of carbon contamination. Diamond-like carbon contamination causes the greatest decrease in reflectivity, and polymer-like carbon causes the smallest decrease. When the thickness of carbon contaminant is 2 nm, the diamond-like carbon reduces reflectivity by 3.87% and the graphitic-like carbon reduces reflectivity by 2.63%. The polymer-like carbon's reflectivity depends on its density ρ: its reflectivity decreases by 1.4% for $\rho = 1.25$ g/cm^3 and 0.94% for $\rho = 0.9$ g/cm^3. When the thickness of carbon contaminant is 5 nm, the differences in reflectivity are more pronounced than for 2 nm thickness, but the trend of reflectivity decreases is still the same. The reflectivity losses are 11.21%, 6.93%, 3.87% and 2.75% for diamond-like, graphitic-like and polymer-like carbon with different densities, respectively.

In summary, these curves display the relationship between the different carbon contamination types and their associated reflectivity losses. Therefore, the carbon type can be estimated according to the thickness and reflectivity loss of the carbon layer.

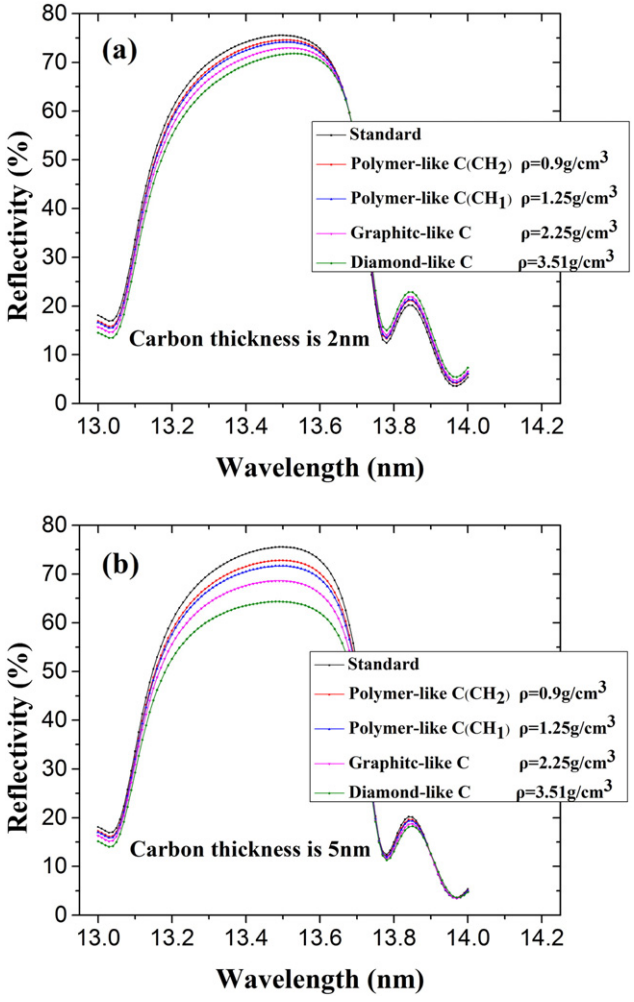

Fig. 1. The dependence of reflectivity value of multilayers on the types of carbon contamination (a) 2 nm thickness of carbon (b) 5 nm thickness of carbon.

3. The mechanism of atomic hydrogen cleaning

Physical sputtering and chemical reactions work simultaneously in cleaning process, and they have been offered as explanations for the mechanisms of various cleaning methods. However, the basic chemical kinetics mechanism for atomic hydrogen cleaning technology is not clear for each of the different types of carbon contamination [11]. Therefore, further research of the cleaning mechanism is necessary to build the cleaning model.

3.1. Physical sputtering

The mechanism of physical sputtering is the process in which the incident hydrogen atoms impact with high energy on the surface of the EUV multilayer and transfer their energy to carbon atoms. When the carbon atoms absorb sufficient energy to overcome the surface binding energy E_s, they will escape from the surface. The physical sputtering yield is calculated by simulation software [12]. Fig. 2 shows the relationship between physical sputtering yield and the energy of incident hydrogen atoms for different types of carbon contamination.

The energy threshold E_{th} for different types can be obtained from Fig. 2. This figure shows that E_{th} depends on the type of carbon contamination. The E_{th} of polymer-like carbon is lower than that of other carbon types. The higher the hydrogen concentration in polymer-like carbon contaminants is, the smaller E_{th} is. Because CH_3– is not stable, CH_2– has the highest hydrogen concentration of polymer-like carbon contaminants. It means that the E_{th} for CH_2– is the smallest. The energy of incident atomic hydrogen generated by heating a W-filament is lower than the smallest E_{th} in most cases. Therefore, the physical sputtering contributes minimally to the cleaning process.

3.2. Chemical reaction

Because physical sputtering has been shown to be a minor factor, a chemical reaction is thus the main mechanism of atomic hydrogen cleaning technology to remove carbon contaminants. A mathematical model considering the chemical reaction is built to accurately describe the reaction between atomic hydrogen and carbon. It consists of two parts: the transport of atomic hydrogen and the chemical reaction itself.

Atomic hydrogen is produced by a high temperature W-filament. It is not stable and will recombine to hydrogen during the transport process [13]. To simulate the flux of atomic hydrogen that arrives at the surface of multilayer, the Arrhenius function is used here. k_h^- stands

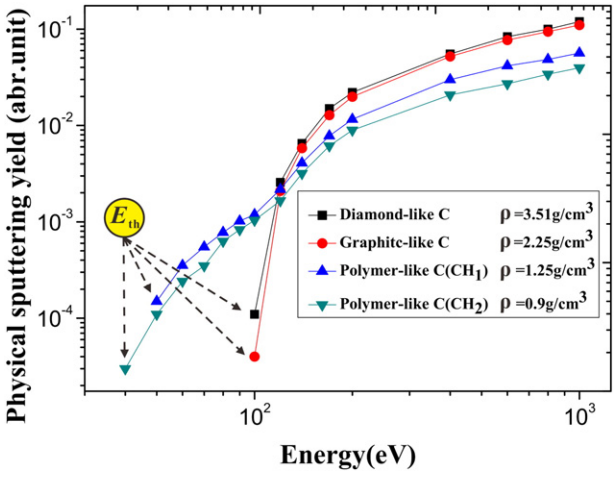

Fig. 2. The dependence of physical sputtering yield for different types of carbon contamination on the energy of incident hydrogen atoms.

for the rate of recombination and depends on T. The expression is described as:

$$k_{h^-} = \alpha \exp\left(\frac{-E_b}{k_B T}\right), \tag{1}$$

where α is a pre-exponential factor, k_B is the Boltzmann constant, and E_b is the activation energy for hydrogen recombination [14].

As conservation of the amount of hydrogen is required, the equilibrium equation between incident hydrogen and hydrogen desorption is written as [15]:

$$n_H k_{h^-} = \varphi\left(1 - \frac{n_H}{n_0}\right), \tag{2}$$

where n_H is the concentration of atomic hydrogen at surface. n_0 is the saturated concentration on the surface of carbon layer. To protect the multilayer, the substrate temperature is lower than 370 K in cleaning process, in which situation n_0 is a constant (1.0×10^{16} cm^{-2}) [16]. φ is the incident atomic hydrogen flux density, and it can be depicted as: $\varphi = (I \times sr)/[(2000\ \mathrm{K}/T)^{1/2} \times S \times d^2]$. Here I is the atomic ion current detected by a quadrupole mass analyzer, sr is the angular distribution of atomic hydrogen, S is the sensitivity factor, and d is the working distance between the atomic hydrogen source and the sample [17]. And therefore the atomic hydrogen concentration is written as:

$$n_H = n_0 \frac{\varphi}{\varphi + n_0 k_{h^-}}. \tag{3}$$

According to the Eq. (3), n_H is dependent on the rate of recombination and the incident atomic hydrogen flux.

As for the process of the chemical reaction, the active atomic hydrogen combines with atomic carbon by a chemical reaction, first producing volatile hydrocarbon, which later escapes to the surrounding atmosphere [15,18–19]. The cleaning rate is described by the change of carbon thickness, and it is described in the model as:

$$\frac{dD_c}{dt} = R \times n_c \times l_c \times \left(\frac{1}{N_c}\right) \tag{4}$$

where D_c denotes the carbon thickness, dD_c/dt denotes the cleaning rate, and R is reaction rate. n_c is the required number of carbon atoms in the hydrocarbon, and it is equal to 1, because the volatile hydrocarbon is commonly CH_x ($x = 2$, 3 and 4). l_c is the thickness of a single layer of carbon atoms. N_c is the number of carbon atoms per unit area. It is assumed that the carbon atom is a cube and the atoms are closely arranged. Thus, l_c and N_c can be written respectively as:

$$l_c = V^{\frac{1}{3}} = \left(\frac{M}{\rho N_A}\right)^{\frac{1}{3}}, \tag{5}$$

$$N_c = \frac{1}{l_c^2}, \tag{6}$$

where M is the carbon atom molar mass, ρ is the density of the carbon layer, and N_A is the Avogadro constant.

According to the kinetic theory of chemical reactions, the reaction rate is described as:

$$R = n_H k = n_H \beta \times T^{(m)} \exp\left(\frac{-E_a}{k_B T}\right), \tag{7}$$

where k is the Arrhenius function, β is a pre-exponential factor, and T is the substrate temperature. E_a is the activation energy of the reaction between carbon and hydrogen atoms, which relies on T and can be corrected by $T^{(m)}$. β, m and E_a can be obtained by fitting the experimental data. According to Eqs. (3)–(7), the cleaning rate is written as:

$$\frac{dD_c}{dt} = n_0 \frac{\varphi}{\varphi + n_0 \alpha \exp\left(\frac{-E_b}{k_B T}\right)} \times \beta \times T^{(m)} \exp\left(\frac{-E_a}{k_B T}\right) \times n_c \times V. \tag{8}$$

Therefore, the mathematical model for cleaning different carbon contamination types is established. A database of β and E_a for different types will be produced by model and experimental data. The model is useful for choosing the best conditions for removing the carbon contaminants and predicting the appropriate cleaning time.

4. Results and discussion

In order to verify the proposed model, this paper compares values calculated by the model with experimental data from the literature [5,20]. In literature [20], there are three types of carbon contaminants induced by EUV, hot filament and PVD, respectively. And the parameters of each type are shown in the Table 1. The hydrogen is cracked by a W-filament at temperature of 2270 K, the flow of hydrogen is 3 sccm, and the distance between the atomic hydrogen source and the surface of sample is 4 cm. The values of β and E_a in Table 1 are calculated by a nonlinear regression function. The dependence of the cleaning rate on the substrate temperature T, for the calculations and the experimental data, are shown in Fig. 3.

In literature [5], the contaminants are graphite-like and are induced by sputtering. Atomic hydrogen is generated in the same way as [20]. The power of W-filament is 378 W, the pressure of hydrogen is 0.9 mTorr, and the substrate temperature is 320 K. The working distance d varies from 200 mm to 500 mm. And the values of β and E_a are also calculated by a nonlinear regression function. The dependence of the cleaning rate on the working distance d, for the calculations and the experimental data, are shown in Fig. 4.

Fig. 3 and Fig. 4 illustrate the calculated values and experimental data of cleaning rates at different conditions in literatures [5,20]. Overall, the calculated cleaning rates are in good agreement with the experimental data. Having compared the calculations of the cleaning rate with available experimental data, we now evaluate the effects of key parameters in the model. These parameters include the types of carbon contamination, substrate temperature T, and activation energy E_a. Then the effects of these parameters are analyzed and shown in Fig. 5.

According to Fig. 5 (a) and Fig. 5 (b), the cleaning rate decreases when the density of the carbon layer increases. For instance, the cleaning rate decreases from 0.316 nm/min to 0.266 nm/min when the density increases from 0.9 g/cm^3 to 1.4 g/cm^3 at 340 K for a polymer-like carbon. And the rate for polymer-like carbon contamination is higher than for others in the same situation. For instance, at 340 K, the cleaning rate of the polymer-like carbon layer with a density of 1.2 g/cm^3 is 0.287 nm/min, while the rates for graphite-like carbon layers with densities of 2.0 g/cm^3 and 2.2 g/cm^3 are 0.025 nm/min and 0.053 nm/min, respectively.

Table 1
The parameters of different types of carbon contamination.

Parameters	EUV	Hot filament	PVD
β	2.08×10^1	3.35×10^{-3}	8.65×10^{-1}
E_a(eV)	0.45	0.26	0.40
sp^3/sp^2	10.2	0.7	0.5
Density(g/cm^3)	1.2	2.0	2.2
Carbon type	Polymer-like	Graphite-like	Graphite-like

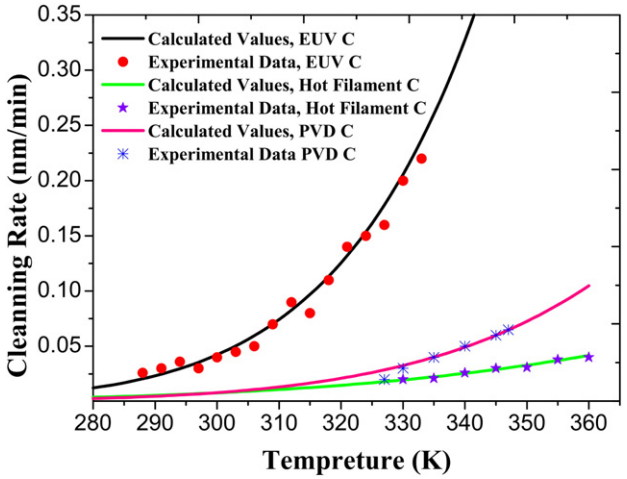

Fig. 3. The dependence of the calculating and experimental cleaning rate on the substrate temperature *T*.

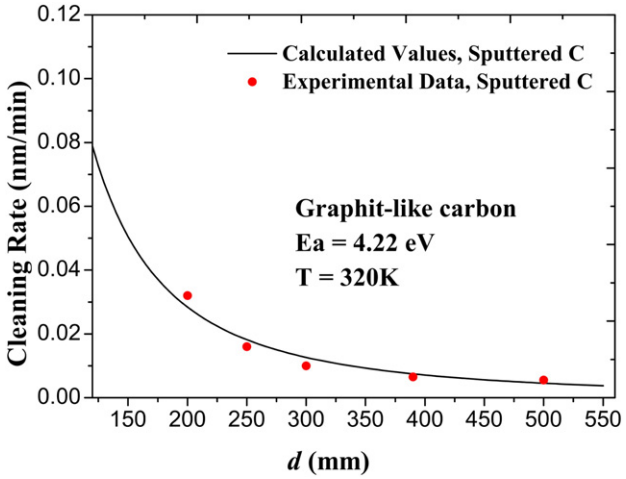

Fig. 4. The dependence of the calculating and experimental cleaning rate on the working distance *d*.

Fig. 5 (c) and Fig. 5 (d) show how the cleaning rate depends on the activation energy for different types of carbon contamination, and the cleaning rate declines exponentially as activation energy increases. In addition, Fig. 5 (d) also shows that although the two types of carbon contamination are both graphitic-like carbon, the E_a and cleaning rate are different, which means different mechanisms are involved for different structures of carbon layers. The cleaning rate for PVD carbon is higher than for hot filament carbon by an order of magnitude.

Based on the comparison analysis above, the atomic hydrogen cleaning rates are different for various types of carbon contamination. The cleaning rate for hydrogen-filled contaminant is much higher than for other contaminants. This difference is caused by the two different processes in the chemical reaction: carbon atomic hydrogenation and chemical erosion [20,21].

For carbon contaminants without hydrogen, the orbital hybridization state of carbon atom is sp^2. When the atomic hydrogen arrives at the surface, the hydrogenation process occurs and the state of orbital hybridization changes from sp^2 to sp^3. Volatile hydrocarbons are generated after the hydrogenation process, and the orbital hybridization state becomes sp^3. The hydrocarbons escape later from the surface when it absorbs enough energy from collision and reaction to overcome the surface binding energy. This process is described in Fig. 6. Thus, carbon contaminants could be removed from the surface of EUV multilayers by repeating the above process. This mechanism can explain why the cleaning rates vary with carbon types. The carbon atoms in polymer-like carbon are mostly in the sp^3 orbital hybridization state while the carbon atoms in other types of carbon are mostly in the sp^2. Therefore, the process of cleaning polymer-like carbon requires minimal hydrogenation; therefore, it would take less time to remove this type of contaminants than to remove other types. Both the type of carbon and the structure of carbon affect the cleaning rate.

5. Conclusions

Atomic hydrogen is used to remove carbon contaminants on multilayers used for extreme ultraviolet lithography. In this paper, which focuses on the atomic-hydrogen-based carbon contamination cleaning process, a possible mechanism for the associated reactions is studied, and a cleaning model is established. The calculated values are in good agreement with the existing experimental data in the literature. Moreover, the influences of the main factors – such as activation energy and types of carbon contamination – on the cleaning rate are discussed by proposed model. The results show that the cleaning rate depends on the types of contamination, which is well explained by analyzing the different processes involved in chemical reaction for cleaning different types of contamination. The proposed model could be used to effectively predict and evaluate the cleaning rates for different carbon contamination types.

Acknowledgments

This work was funded by the National Nature Science Foundation of China (No. 61404139), the National Science and Technology Major Project (No. 2012ZX02702001-005), the Independent fund of State Key Laboratory of Applied Optics (Y5743FQ158), and the Key Science and Technology Achievements Transformation Projects of Jilin Province (20150307039GX).

References

[1] O. Wood, C.-S. Koay, K. Petrillo, H. Mizuno, S. Raghunathan, J. Arnold, D. Horak, M. Burkhardt, G. Mclntyre, Y. Deng, B.L. Fontaine, U. Okoroanyanwu, EUV lithography at the 22 nm technology node, Proc. SPIE 7636 (2010) 297–301.
[2] B. Wu, Next-generation lithography for 22 and 16 nm technology nodes and beyond, Sci. China Inf. Sci. 54 (2011) 959–979.
[3] L.H. Wang, X.K. Wang, B. Chen, Study for dual-function EUV multilayer mirror, Opt. Laser Technol. 40 (2008) 571–574.
[4] X. Gong, Q. Lu, G. Lu, Establishment of theoretical model and experimental equipment for researching on carbon contamination of EUV multi-layer mirror, Proc. SPIE 9446 (2015) 94460W.
[5] S. Graham, C.A. Steinhaus, W.M. Clift, L.E. Klebanoff, S. Bajt, Atomic hydrogen cleaning of EUV multilayer optics, Proc. SPIE 5037 (2003) 460–469.
[6] K. Motai, H. Oizumi, S. Miyagaki, I. Nishiyama, A. Izumi, T. Ueno, Y. Miyazaki, A. Namiki, Atomic hydrogen cleaning of Ru-capped EUV multilayer mirror, Proc. SPIE 6517 (2007) 65170F.
[7] K. Motai, H. Oizumi, S. Miyagaki, I. Nishiyama, A. Izumi, T. Ueno, A. Namiki, Cleaning technology for EUV multilayer mirror using atomic hydrogen generated with hot wire, Thin Solid Films 516 (2008) 839–843.
[8] E. Strein, D. Allred, Eliminating carbon contamination on oxidized Si surfaces using a VUV excimer lamp, Thin Solid Films 517 (2008) 1011–1015.
[9] J. Chen, E. Louis, H. Wormeester, R. Harmsen, R. Kruijs, C.J. Lee, W. Schaik, F. Bijkerk, Carbon-induced extreme ultraviolet reflectance loss characterized using visible-light ellipsometry, Meas. Sci. Technol. 22 (2011) 880–897.
[10] E. Louis, A.E. Yakshin, P.C. Goerts, S. Oestreich, E.L. Goerts, M. Kessels, D. Schmitz, F. Scholze, G. Ulm, S. Muellender, M.H. Haidl, F. Bijkerk, Mo/Si multilayer coating technology for EUVL: coating uniformity and time stability, Proc. SPIE 4146 (2000) 60–63.
[11] E. Pellegrin, I. Šics, J. Reyes-Herrera, C.P. Sempere, J.J.L. Alcolea, M. Langlois, J.F. Rodriguez, V. Carlino, Characterization, optimization and surface physics aspects of in situ plasma mirror cleaning, J. Synchrotron Radiat. 21 (2014) 300–314.
[12] R.E.H. Clark, D.H. Reiter, Nuclear Fusion Research: Understanding Plasma-Surface Interactions, Springer-Verlag, Berlin Heidelberg, Netherlands, 2005.
[13] E. Molinari, M. Tomellini, Non-equilibrium vibrational kinetics and 'hot atom' models in the recombination of hydrogen atoms on surfaces, Chem. Phys. 270 (2001) 439–458.

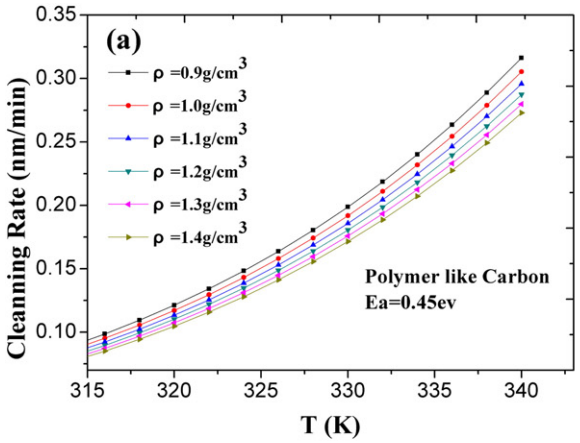

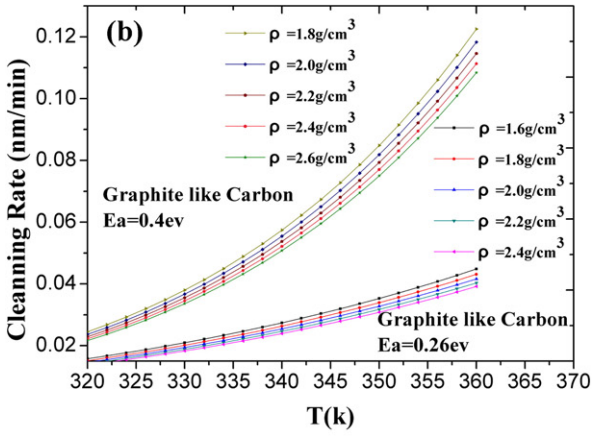

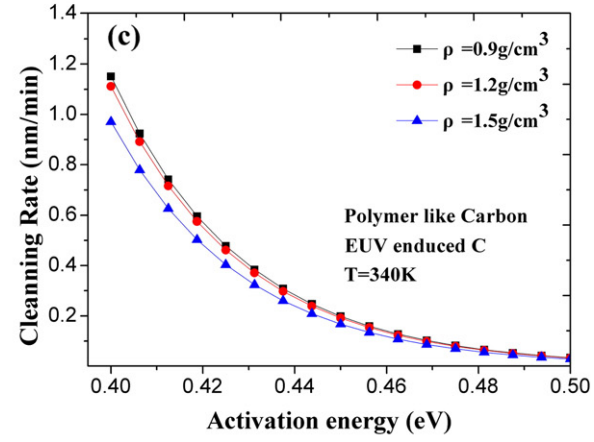

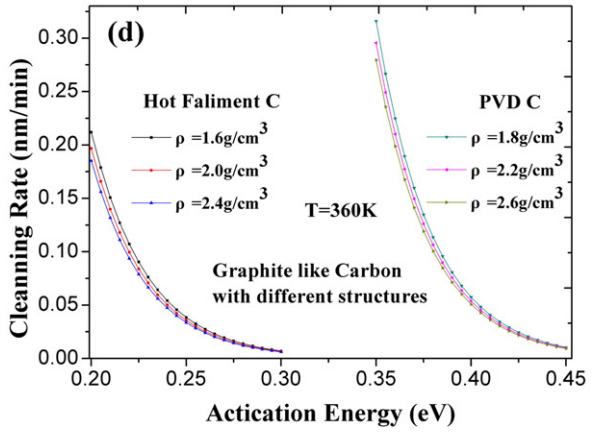

Fig. 5. The curves of cleaning rate (a) for polymer-like carbon under different T and ρ. (b) for different graphite-like carbon for structures under different T and ρ. (c) for polymer-like carbon under different activation energy at 340 K. (d) for different graphite-like carbon for structures under different activation energy at 360 K. β and E_a are quoted from Table 1.

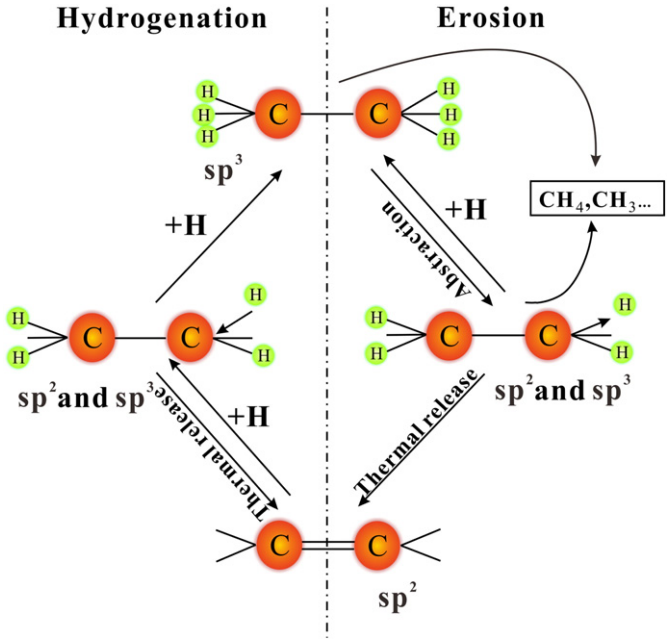

Fig. 6. The process of chemical reaction mechanism.

[14] J.W. Davis, A.A. Haasz, Impurity release from low-Z materials under light particle bombardment [J], J. Nucl. Mater. 241 (1997) 37–51.
[15] C.M. Donnelly, R.W. Mccullough, J. Geddes, Etching of graphite and diamond by thermal energy hydrogen atoms, Diam. Relat. Mater. 6 (1997) 787–790.
[16] S.K. Erents, Methane formation during the interaction of energetic protons and deuterons with carbon, J. Nucl. Mater. 63 (1976) 399–404.
[17] K.G. Tschersich, J.P. Fleischhauer, H. Schuler, Design and characterization of a thermal hydrogen atom source, J. Appl. Phys. 104 (2008) 034908.
[18] J. Roth, C. García-Rosales, Analytic description of the chemical erosion of graphite by hydrogen ions, Nucl. Fusion 36 (1996) 1647–1659.
[19] J. Chen, C.J. Lee, E. Louis, F. Bijkerk, R. Kunze, H. Schmidt, D. Schneider, R. Moors, Characterization of EUV induced carbon films using laser-generated surface acoustic waves, Diam. Relat. Mater. 18 (2009) 768–771.
[20] J. Chen, E. Louis, R. Harmsen, T. Tsarfati, H. Wormeester, M.V. Kampen, W.V. Schaik, R.V.D. Kruijs, F. Bijkerk, In situ ellipsometry study of atomic hydrogen etching of extreme ultraviolet induced carbon layers, Appl. Surf. Sci. 258 (2011) 7–12.
[21] J. Roth, Chemical erosion of carbon based materials in fusion devices, J. Nucl. Mater. 266 (1999) 51–57.